A bed-load transport model for rough turbulent open-channel flows on plane beds

Athol D. Abrahams[1]* and Peng Gao[2]

[1] *Department of Geography, University at Buffalo, The State University of New York, Buffalo, NY 14261, USA*
[2] *Department of Geography, Syracuse University, Syracuse, NY 13244, USA*

**Correspondence to:
A. D. Abrahams, Department
of Geography, University at
Buffalo, The State University
of New York, Buffalo, NY
14261, USA. E-mail:
abrahams@buffalo.edu*

Abstract

Data from flume studies are used to develop a model for predicting bed-load transport rates in rough turbulent two-dimensional open-channel flows moving well sorted non-cohesive sediments over plane mobile beds. The object is not to predict transport rates in natural channel flows but rather to provide a standard against which measured bed-load transport rates influenced by factors such as bed forms, bed armouring, or limited sediment availability may be compared in order to assess the impact of these factors on bed-load transport rates. The model is based on a revised version of Bagnold's basic energy equation $i_b s_b = e_b \omega$, where i_b is the immersed bed-load transport rate, ω is flow power per unit area, e_b is the efficiency coefficient, and s_b is the stress coefficient defined as the ratio of the tangential bed shear stress caused by grain collisions and fluid drag to the immersed weight of the bed load. Expressions are developed for s_b and e_b in terms of G, a normalized measure of sediment transport stage, and these expressions are substituted into the revised energy equation to obtain the bed-load transport equation $i_b = \omega G^{3\cdot4}$. This equation applies regardless of the mode of bed-load transport (i.e. saltation or sheet flow) and reduces to $i_b = \omega$ where G approaches 1 in the sheet-flow regime. That $i_b = \omega$ does not mean that all the available power is dissipated in transporting the bed load. Rather, it reflects the fact that i_b is a transport rate that must be multiplied by s_b to become a work rate before it can be compared with ω. It follows that the proportion of ω that is dissipated in the transport of bed load is $i_b s_b / \omega$, which is approximately 0·6 when $i_b = \omega$. It is suggested that this remarkably high transport efficiency is achieved in sheet flow (1) because the ratio of grain-to-grain to grain-to-bed collisions increases with bed shear stress, and (2) because on average much more momentum is lost in a grain-to-bed collision than in a grain-to-grain one. Copyright © 2006 John Wiley & Sons, Ltd.

Keywords: sediment transport; bed-load transport; saltation; sheet flow

Introduction

In this paper we present a model for predicting bed-load transport rates in two-dimensional open-channel flows over plane beds. The purpose of this model is to provide a standard against which measured bed-load transport rates in flows subject to influences such as bed forms, bed armouring, and limited sediment availability may be compared to assess the impact of these influences on bed-load transport rates. More specifically, the model is developed for sediment-laden flows that meet the following requirements: (1) the flow is steady, uniform, two-dimensional, turbulent, and hydrodynamically rough; (2) the bed is plane and mobile and comprises non-cohesive natural sediments that are well sorted and similar in shape; (3) the sediment in transport is the same as that forming the bed; and (4) the sediment is readily available, enabling bed load to be transported at capacity (i.e. at the maximum possible rate). The end-product of the model is an equation that predicts bed-load transport rates on plane beds whether the bed load moves mainly by saltation (i.e. in the saltation regime) or by sheet flow (i.e. in the sheet-flow regime).

Whether saltation or sheet flow is the dominant mode of bed-load transport depends on the dimensionless bed shear stress

$$\theta = \frac{\tau}{gD(\rho_s - \rho)} \tag{1}$$

where $\tau = \rho g h S$ is the total shear stress applied to the bed, g is the acceleration of gravity (m s^{-2}), h is the flow depth (m), S is the energy slope, ρ is the density of the fluid (kg m^{-3}), ρ_s is the density of the sediment (kg m^{-3}), and D is the median grain diameter (m). As bed shear stress increases the mode of bed-load transport changes from saltation to sheet flow. The term saltation refers to the hopping or jumping of grains over the bed; but in this paper, for convenience, it also includes rolling and sliding, which are viewed as incipient forms of saltation (Bagnold, 1973). At low bed shear stress ($\theta < 0.1$), saltating grains are widely spaced and rarely collide with other saltating grains (Leeder, 1979a). Thus intergranular collisions are mainly grain-to-bed (GB). As bed shear stress increases, grain concentration increases and collisions between saltating grains become more common. Consequently, at medium bed shear stress ($0.1 \leq \theta < 0.5$) intergranular collisions are predominantly grain-to-grain (GG) (Leeder, 1979a; Sumer *et al.*, 1996).

Finally, at high bed shear stress ($0.5 \leq \theta$), sheet flow occurs on upper-regime plane beds (e.g. Engelund and Hansen, 1967; Nnadi and Wilson, 1995; Sumer *et al.*, 1996). When there is no suspended sediment, sheet flow consists of a layer of colliding grains with a basal concentration approaching that of the stationary bed (i.e. a concentration of about 0.65) (Bagnold, 1956; Pugh and Wilson, 1999). Gao (2003) used high-speed video (at 500 frames per second) to study the internal structure of sheet flow. Like Wang and Chien (1987), Gao (2003) observed that in addition to saltating, grains travel in poorly defined granular sheets that slide or roll over the slower moving sheets below. Wang and Chien (1987) and Gao (2003) referred to these sheets as laminations and attributed them to the dilation and downstream movement of one or more layers of grains that formerly defined the bed surface. Indeed, it is evident that the bed-load transport rate in the sheet-flow regime is controlled by a self-adjusting mechanism in which the immersed weight of the bed load that can be dilated and transported downslope by the shearing flow is balanced by a normal dispersive stress that arises from collisional interactions.

Bagnold (1956, 1966) argued that in sheet flow the normal dispersive stress that supports the bed load is generated more or less entirely by intergranular collisions. In contrast, Bridge (2003, p. 60) and his colleagues (e.g. Bridge and Bennett, 1992) have argued that in addition to grain collisions, turbulent fluid lift plays a significant role in supporting the bed load. Given that high grain concentrations at the base of the bed-load layer suppress turbulence and hence fluid lift (e.g. Middleton and Southard, 1984, p. 230; Wijetunge and Sleath, 1998), most investigators (e.g. Leeder, 1979b; Engelund, 1981; Hanes and Bowen, 1985; Wilson, 1987; Wang and Chien, 1987; Nnadi and Wilson, 1992; Fredsoe, 1993; Jenkins and Hanes, 1998) agree with Bagnold (1956, 1966) that in the sheet-flow regime, fluid lift at the base of the bed-load layer is inconsequential and the bed load is supported more or less entirely by a normal dispersive stress generated by grain collisions.

According to Bagnold (1966, 1973), a fluid flow is a transporting machine, the performance of which is described by the basic energy equation

$$i_b \tan \alpha = e_b \omega \qquad (2)$$

where $i_b = q_b g(\rho_s - \rho)$ is the immersed bed-load transport rate (J s^{-1} m^{-2}), q_b is the volumetric bed-load transport rate (m^2 s^{-1}), $\tan \alpha$ is the dynamic friction coefficient, e_b is the efficiency of bed-load transport, $\omega = u\tau$ is the flow power per unit bed area (W m^{-2}), and u is the mean flow velocity (m s^{-1}). The left side of Equation 2 represents the rate of doing work transporting bed load per unit area of the bed (J s^{-1} m^{-2}), whereas the right side indicates the power expended on bed-load transport over the same area (W m^{-2}).

Bagnold (1954, 1956, 1966, 1973) defined $\tan \alpha$ as the ratio of the tangential bed shear stress to the normal stress arising from grain collisions with the bed. According to Bagnold (1956, 1966, 1973), the immersed weight of the bed load is supported entirely by the normal component of the dispersive stress produced by intergranular collisions. However, there is now good evidence to suggest that at low shear stress fluid drag contributes to the tangential stress that drives the bed load downstream (Fernandez Luque and van Beek, 1976), while fluid lift contributes to the normal stress that supports the bed load in motion (e.g. Leeder, 1979b; Bridge and Bennett, 1992; Nino *et al.*, 1994; Nino and Garcia, 1994, 1998a, b; McEwan *et al.*, 1999; Seminara *et al.*, 2002). Inasmuch as $\tan \alpha$ does not take either fluid lift or fluid drag into account, Bagnold's (1966, 1973) energy equation is revised by replacing $\tan \alpha$ with a new coefficient termed the stress coefficient s_b. Equations are then developed for s_b and e_b and substituted into the revised energy equation to obtain the bed-load transport equation.

Data

The selection of data for developing and testing the bed-load transport model was guided by the model requirements listed above. To comply with the last requirement that bed-load transport occurs at capacity, only data for flows

through open-channel flumes were included in this study. Flows through natural channels were excluded, as such flows commonly transport bed load below capacity, especially where the channel is eroded in resistant materials and/or has coarse bed sediments (e.g. Nanson, 1974; O'Leary and Beschta, 1981; Meade, 1985; Reid *et al*., 1985; Reid and Frostick, 1986; Gomez, 1991; Reid and Laronne, 1995).

Nine flume studies by Guy *et al*. (1966), Williams (1970), Smart (1984), Graf and Suszka (1987), Aziz and Scott (1989), Rickenmann (1991), Song *et al*. (1998), Gao (2003) and Gao and Abrahams (2004) were identified in which fully rough turbulent flows were transporting well sorted non-cohesive sediments over mobile plane beds. Flows were considered to be turbulent and fully rough if the flow Reynolds number $R_h = 4hu/v > 8000$ and the roughness Reynolds number $R_{ks} = k_s u_*/v > 70$, where v is the kinematic viscosity (m^2 s^{-1}), $u_* = (ghS)^{0.5}$ is the shear velocity (m s^{-1}), $k_s = mD$ is the equivalent sand roughness (m), and m is a coefficient which is assumed to be 3 (e.g. van Rijn, 1982; Yen, 1991, table 12).

In these nine studies a total of 365 experiments satisfied the above requirements. However, 43 of these experiments, including all those by Guy *et al*. (1966), were discarded because their flows were transporting significant amounts of suspended sediment. These flows were identified by specifying the threshold value W_t of the dimensionless settling velocity $W = w/u_*$ at which suspension commences (Sumer *et al*., 1996), where w is the mean settling velocity of the grains (m s^{-1}) (Cheng, 1997). Cheng and Chiew (1999) reviewed the literature on the initiation of suspension in the saltation regime and found that the criteria W_t ranged from 1·25 (Bagnold, 1966) to 2·5 (van Rijn, 1984b). Bridge (2003, pp. 56–57) also reviewed the literature on this topic from a turbulence perspective and concluded that W_t ranges from about 1·2 to 1·5. On the basis of these two reviews, we adopted $W_t = 1·5$ as the criterion for suspension in the saltation regime.

Sumer *et al*. (1996) conducted an extensive set of experiments in the sheet-flow regime and concluded that suspension begins when W falls below 0·8 to 1. Abrahams (2003) analysed data from 155 flume experiments in the sheet-flow regime and found that suspension commences when $W \approx 0·8$. Evidently, suspension in the saltation regime starts at a larger value of W than it does in the sheet-flow regime. This notion is consistent with Pugh and Wilson's (1999) finding that turbulent damping occurs in the sheet-flow regime. Turbulent damping reduces the mean upward-directed turbulent velocity associated with a particular value of u_*, making it possible for suspension to occur at a smaller value of $W = w/u_*$ than if there were no damping. On the basis of these findings, we selected $W_t = 0·8$ as the suspension criterion in the sheet-flow regime.

The existence of different suspension criteria for the saltation and sheet-flow regimes means that every flow must be assigned to one regime or the other. As noted above, the variable most often used for this purpose is θ. The threshold value of θ at which the saltation regime is replaced by the sheet-flow regime θ_t coincides with the transition from washed out dunes to upper-regime plane beds. There is no single value for θ_t. Instead there is a range of values extending from about 0·5 to 1 over which one finds examples of both regimes (e.g. Engelund and Hansen, 1967; Hill *et al*., 1969; van Rijn, 1984c; Allen, 1985, p. 72; Wang and White, 1993; Nnadi and Wilson, 1995; Sumer *et al*., 1996). In the absence of any compelling reason for selecting one value for θ_t rather than another, θ_t was set equal to 0·5 and this value is used throughout the study.

The final data set consists of 322 flume experiments. These experiments were performed in flumes of different sizes (Table I). Where flumes are not sufficiently wide, sidewall drag has a significant effect on flow hydraulics. It is therefore necessary to remove this effect in order to compare or combine data from different flumes and to meet the requirement of two-dimensional flow. Consequently, all flume experimental data were corrected for sidewall drag by Williams' (1970) method, which uses flow depth and corrects the slope rather than the hydraulic radius.

The 322 experiments in the data set were conducted on slopes β ranging from 0·057° to 11·3°. As β increases, the downslope component of gravity increases, thereby facilitating the transport of bed sediments. To include this effect in a bed-load transport equation, the conventional slope variable $S = \sin \beta$ was divided by $\sin (\phi_r - \beta)/\sin \phi_r$, where $\phi_r = 32°$ is the residual angle of repose for the grains in transport (Schoklitsch, 1914; van Rijn, 1993, pp. 4·11, 7·29). Thus, S varies from 0 to ∞ as β varies from 0 to ϕ_r.

Finally, it is necessary to determine for each experiment the critical value of θ at which bed sediments begin to move θ_c. This variable is notoriously difficult to evaluate (e.g. Buffington and Montgomery, 1997). In Williams' (1970), Graf and Suszka's (1987) and Song *et al*.'s (1998) 182 experiments, θ_c was estimated by plotting the volumetric bed-load transport rate q_b against θ, fitting trendlines to the data, and extending these trendlines to the θ axis where $q_b = 0$. In the remaining 140 experiments by Smart (1984), Aziz and Scott (1989), Rickenmann (1991), Gao (2003) and Gao and Abrahams (2004), the smallest values of q_b were too large to give trustworthy estimates of θ_c by the extrapolation procedure. Consequently, in these 140 experiments θ_c was set equal to 0·04, which is close to the mean of 0·041 for the 182 experiments in which θ_c was measured. Actually, the value assigned to θ_c was of little consequence, as θ was generally so much larger than θ_c that an error in the order of ±0·01 in θ_c has a negligible effect on θ_c/θ and, hence, on the predicted bed-load transport rate.

Table I. Range of data for relevant variables from each source

Variable	Williams (1970)	Smart (1984)	Graf and Suszka (1987)	Aziz and Scott (1989)	Rickenmann (1992)	Gao (2003)	Gao and Abrahams (2004)	Total
Flume length and width (m)	15·8 × 0·6	5·0 × 0·2	16·8 × 0·6	3·7 × 0·23	5·0 × 0·2	12·5 × 0·1	12·5 × 0·1	
Number of experiments	23	37	105	25	49	13	16	322
u (m s^{-1})	0·332–2·338	0·665–1·989	0·917–1·539	0·281–0·539	1·070–2·750	1·900–2·448	0·648–1·391	0·281–2·750
h (m)	0·030–0·154	0·019–0·079	0·066–0·201	0·004–0·012	0·044–0·090	0·020–0·087	0·026–0·071	0·004–0·201
R_h	34 285–522 832	91 666–540 716	230 057–1 236 641	8871–19 275	144 843–638 112	422 404–783 273	58 769–300 871	8871–1 236 641
R_{ks}	38–174	562–4483	1005–4465	32–82	1382–3175	139–155	105–830	32–4483
$Fr*$	0·50–3·9	1·09–2·89	0·84–1·30	1·18–2·57	1·56–2·99	0·84–2·73	1·28–2·92	0·50–3·9
S	0·001–0·024	0·032–0·293	0·005–0·025	0·031–0·118	0·079–0·293	0·005–0·031	0·027–0·032	0·001–0·293
D (× 10^{-3} m)	1·35	4·2, 10·5	12·2, 23·5	0·51–1·02	10	1·16	1·16, 7	0·51–23·5
θ	0·033–1·097	0·097–1·54	0·033–0·084	0·151–0·658	0·257–1·83	0·863–1·14	0·073–0·606	0·033–1·83
i_b (J s^{-1} m^{-2})	0·002–28·48	2·151–458·3	0·004–3·206	0·262–4·679	20·68–574·6	17·89–34·92	0·158–8·669	0·002–574·6
ω (W m^{-2})	0·36–56	20·8–345·1	7·0–45·0	0·95–5·75	47–741·1	30·7–53·2	5·36–23·1	0·36–741·1
W	0·846–4·13	0·852–3·54	3·81–6·02	0·810–2·25	0·802–2·16	0·816–0·952	1·13–4·00	0·802–6·02

* Froude number $Fr = u/(gh)^{0.5}$.

Not only is the transport of bed sediments facilitated by the downslope component of gravity, but so is their entrainment. Accordingly, for the flume experiments the estimated value of θ_c was corrected for this effect by multiplying it by $\sin(\phi_r - \beta)/\sin\phi_r$ (e.g. Chiew and Parker, 1994; Lau and Engel, 1999; Graf, 2000; Whitehouse *et al.*, 2000).

The 322 flume flows in the present data set represent a wide range of conditions that encompass both the saltation and sheet-flow regimes. This range of conditions is all the more remarkable when one considers that the upper limit for many variables (e.g. h, S, θ) is constrained by the requirement that the flow transports only bed load (i.e. more powerful flows cannot be included as they transport a significant amount of sediment in suspension). Table I lists the range of values for each experimental variable and the dimensions of the flume used in each study. For additional information on the experimental apparatus and procedures, the original references should be consulted.

Model

Tan α relation

In a fluid flow transporting bed load, the steady forward motion of the bed load is opposed by a frictional force caused by intergranular collisions and fluid drag. This friction force is balanced by the total bed shear stress applied by the fluid ($kg\ m^{-1}\ s^{-2}$)

$$\tau = T + \tau_c \tag{3}$$

where T is the tangential bed shear stress ($kg\ m^{-1}\ s^{-2}$) that is required to keep the bed load in motion and τ_c is the critical fluid shear stress ($kg\ m^{-1}\ s^{-2}$) below which bed-load movement ceases. T may be divided into two parts: that part transmitted to the bed by grain collisions and termed grain shear stress T_g ($kg\ m^{-1}\ s^{-2}$), and that part transmitted to the bed by fluid drag and termed fluid shear stress T_f ($kg\ m^{-1}\ s^{-2}$). When all, or nearly all, the shear stress transmitted to the bed is by grain collisions (i.e. $T_g \approx T$), such as occurs in the sheet-flow regime (Bagnold, 1956, 1966), the mean tangential grain stress T_g needed to maintain the bed load in transport is proportional to the immersed weight of the load W' ($kg\ m^{-1}\ s^{-2}$), the proportionality coefficient being

$$\tan\alpha = T_g/W' \tag{4}$$

The value of $\tan\alpha$ is not easily determined. However, data from dry grain flows and various coaxial shearing apparatus indicate that for natural mineral grains in inertial conditions, such as occur at the base of the bed-load layer in the sheet-flow regime (see Bagnold, 1973; Bridge and Bennett, 1992; Bridge, 2003, p. 60; Abrahams, 2003), $\tan\alpha$ can be determined from

$$\tan\alpha = T_g/W' \approx 0.6. \tag{5}$$

This is an important observation, as it suggests that $\tan\alpha$ is always close to 0·6 at high shear stress (i.e. in the sheet-flow regime). At low and medium shear stresses (i.e. in the saltation regime) $\tan\alpha = T_g/W'$ refers to just that part of the tangential stress that is transmitted to the bed by grain collisions. To our knowledge there are no data available on the relative magnitudes of T_g and T_f for mobile beds in the saltation regime. Given (1) that $T_g/W' \approx 0.6$ at high shear stress and (2) that there is considerable uncertainty surrounding the value of T_g/W' at low and medium bed shear stresses, the model assumes that $T_g/W' \approx 0.6$ regardless of bed shear stress. This assumption is simple and plausible and it preserves the mathematical and conceptual simplicity of the model.

The T_g/T relation

Combining Equation 5 with

$$i_b = W'U_b \tag{6}$$

and rearranging terms leads to

$$T_g = T - T_f = \tan\alpha\ W' \approx 0.6W' \approx 0.6i_b/U_b \tag{7}$$

Copyright © 2006 John Wiley & Sons, Ltd.

Earth Surf. Process. Landforms **31**, 910–928 (2006)

where U_b is the mean velocity of the bed-load grains (m s^{-1}). Because i_b is generally known (i.e. measured) for flows transporting bed load at capacity, Equation 7 shows that all that is required to calculate T_g is a knowledge of U_b.

Unfortunately, no data are available on U_b for any experiments in the present data set. Therefore U_b must be calculated from other variables. Although numerous formulas may be found in the literature (e.g. Fernandez Luque and van Beek, 1976; Engelund and Fredsoe, 1982; Bridge and Dominic, 1984; Bridge and Bennett, 1992; van Rijn, 1984a; Sekine and Kikkawa, 1992; Seminara *et al.*, 2002), virtually all of them are based on measurements of grains travelling alone or in small groups over fixed beds and, hence, they overestimate grain velocities in sediment-laden flows over mobile beds (Bagnold, 1966; Wiberg and Smith, 1989; Abrahams and Atkinson, 1993). Only the formula developed by Fernandez Luque and van Beek (1976) is based on data collected entirely from flume flows over mobile beds. However, these authors confined their measurements to flows in which $\theta/\theta_c \leq 2 \cdot 7$ (presumably because tracking individual grains in a cloud of saltating grains becomes increasingly difficult as the concentration of moving grains increases with shear stress.) Consequently, their equation

$$U_b = 9 \cdot 2(u_* - 0 \cdot 7u_{*_c})$$ (8)

applies exclusively to flows that have low bed shear stress.

In the present data set there are 177 flows over mobile beds with $\theta < 0 \cdot 1$, which is equivalent to $\theta/\theta_c < 2 \cdot 7$ if $\theta_c = 0 \cdot 04$. Using Equation 8, U_b was calculated for each flow, and the calculated value of U_b substituted into Equation 7 to obtain the value of T_g for that flow. T_g was then divided by T, and T_g/T was plotted against $1 - (\theta_c/\theta)$ hereafter denoted by G, a normalized measure of sediment transport stage (Figure 1). Logically, when G is close to 0, there is little or no shear stress being transmitted to the bed by moving grains (i.e. $T_g \approx 0$), so $T_g/T \approx 0$ (e.g. Fernandez Luque and van Beek, 1976). On the other hand, when G is close to 1 and there is an abundant supply of sediment (McEwan *et al.*, 1999), the concentration of grains at the base of the bed-load layer approaches that of the stationary bed, the fluid flow is virtually occluded from the bed, and almost all the shear stress is transmitted to the bed by grain collisions (i.e. $T_g \approx T$), so $T_g/T \approx 1$ (e.g. Bagnold, 1956, 1966; Fernandez Luque and van Beek, 1976). In other words, the relation between T_g/T and G is constrained to pass through or very close to the points (0, 0) and (1, 1). For mathematical convenience, we will assume that the relation passes through these points. A power function that both meets this requirement and fits the data well is

$$\frac{T_g}{T} = G^2$$ (9)

This equation is displayed in Figure 1 along with the data from the 177 flume flows over mobile beds.
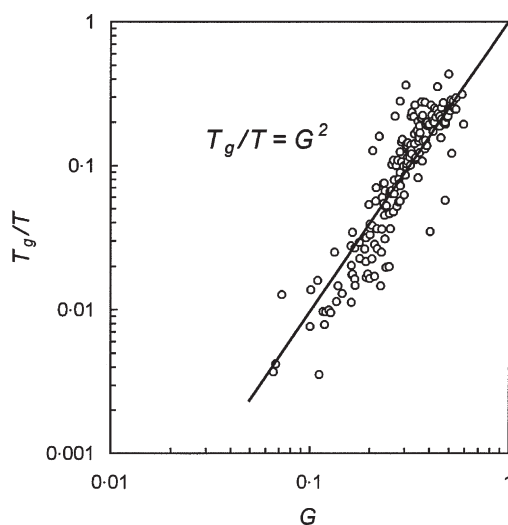
Figure 1. Graph of T_g/T against G for the 177 flows over mobile beds with $\theta < 0 \cdot 1$.

Stress coefficient

Definition. Bagnold (1956, 1966, 1973) postulated that the bed load is supported entirely by a normal stress arising from grain collisions with the bed. Subsequent research has shown that while this may be true at high shear stress (e.g. Wilson, 1987; McEwan *et al.*, 1999), it is not the case at low shear stress, where the bed load is largely supported by fluid lift (e.g. Leeder, 1979b; Nino and Garcia, 1998a, b; Seminara *et al.*, 2002). Furthermore, Figure 1 implies that at low shear stress as G approaches 0, T_f approaches T, and T_g approaches 0 (e.g. Fernandez Luque and van Beek, 1976). Given the roles of fluid lift and fluid drag in bed-load transport, the limitations of tan α become apparent. One way of dealing with this problem is to replace tan α with a new coefficient that includes both T_g and T_f. We term this coefficient the stress coefficient s_b and define it as

$$s_b = \frac{T}{W'} = \frac{T_g + T_f}{W'} \tag{10a}$$

$$s_b = \frac{\tau - \tau_c}{W'} \tag{10b}$$

or

$$s_b = \frac{U_b(\tau - \tau_c)}{i_b} \tag{10c}$$

The revised energy equation then becomes

$$i_b s_b = e_b \omega \tag{11}$$

To derive a bed-load transport equation from Equation 11, functional equations are needed for the coefficients s_b and e_b. In these equations s_b and e_b are related to G, but they are plotted against θ to highlight the fact that both coefficients asymptotically approach 0·6 as θ approaches ∞.

Functional equation. Combining the three equations

$$s_b = \frac{T}{W'} \tag{10a}$$

$$\frac{T_g}{W'} \approx 0 \cdot 6 \tag{5}$$

$$\frac{T_g}{T} = G^2 \tag{9}$$

yields the functional equation

$$s_b = 0 \cdot 6 G^{-2} \tag{12}$$

This equation is plotted in Figure 2 along with the s_b and θ data for the 322 flume experiments. The graph shows that Equation 12 is a good fit to the data where $\theta < 0\cdot1$ but that the data tend to plot above Equation 12 where $\theta \geq 0\cdot1$. This occurs because s_b is calculated using Equation 10c, with U_b in Equation 10c being estimated by Equation 8. As explained above, U_b is estimated by Equation 8 because Equation 8 is based on data from mobile beds. However, such data are available only for flows where $\theta < 0\cdot1$ and intergranular collisions are relatively infrequent. In flows where $\theta \geq 0\cdot1$ intergranular collisions become more frequent and reduce both flow and grain velocities (Wiberg and Smith, 1989; Abrahams and Atkinson, 1993). Consequently, Equation 8 overestimates U_b, and hence s_b, where $\theta \geq 0\cdot1$ (Figure 2). If this line of reasoning is correct, one might expect to find a positive correlation between the bed-load concentration C_b and the degree to which Equation 12 underestimates s_b (i.e. log s_b minus predicted log s_b). As can be seen in Figure 3, such a correlation does in fact exist, though the correlation coefficient is modest ($r = 0\cdot67$). The salient point here is that the tendency in Figure 2 for the points to plot above Equation 12 where $\theta \geq 0\cdot1$ can be explained by our use of Equation 8 to estimate U_b and does not in any way impugn the validity of Equation 12.
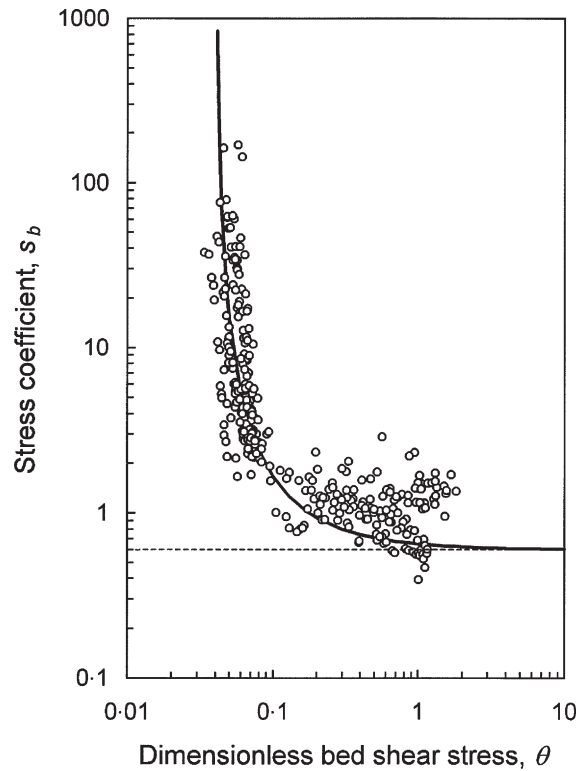
Figure 2. Graph of the stress coefficient against dimensionless bed shear stress. The line is Equation 12. U_b is calculated using Equation 8.
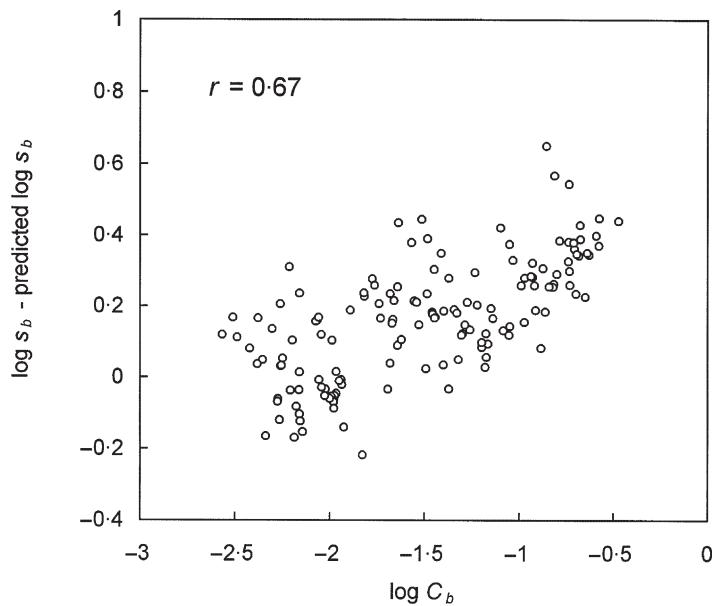
Figure 3. Graph of log s_b − predicted log s_b against log C_b for the 145 flows for which $\theta \geq 0.10$.

Efficiency coefficient

Definition. The efficiency coefficient e_b is the proportion of the flow power or total work rate that is expended transporting bed load at capacity. A general definition for e_b can be obtained by rearranging the revised energy equation (i.e. Equation 11)

$$e_b = \frac{i_b s_b}{\omega} \tag{13a}$$

or

$$e_b = \frac{U_b T}{\omega} = \frac{U_b}{u} \times \frac{T}{\tau} \tag{13b}$$

where $i_b s_b = U_b T$ is the rate of doing work transporting the bed load (J s^{-1} m^{-2}).

Functional equation. Given that $T/\tau = G$, Equation 13b may be written as

$$e_b = \frac{U_b}{u} G \tag{14}$$

which corresponds to the functional equation

$$e_b = a G^b \tag{15}$$

where

$$\frac{U_b}{u} = a G^{b-1} \tag{16}$$

The intercept a is the value of e_b and U_b/u when $G = 1$. Equations 12, 15 and 16 show that when $G = 1$, $s_b = e_b = U_b/u = a = 0\cdot6$. Unlike a, in the present circumstances b cannot be determined algebraically and so must be evaluated statistically.

Values of e_b for the 322 experiments in the data set were computed using Equation 14 and plotted against θ in Figure 4. Because e_b is calculated from Equation 14 which contains U_b, and U_b is obtained from Equation 8 which overestimates U_b where $\theta \geq 0\cdot1$, calculated values of e_b plotted in Figure 4 might be expected to overestimate their true values where $\theta \geq 0\cdot1$ and therefore should not be used to compute the functional equation between e_b and G over this range of θ. However, where $\theta < 0\cdot1$ intergranular collisions are relatively infrequent, and values of e_b calculated from Equation 14 can be used to compute the functional equation.

Thus, the functional equation between e_b and G was obtained by fitting Equation 15 to the data from the 177 experiments where $\theta < 0\cdot1$. This was done by setting the intercept a equal to $0\cdot6$ (Abrahams, 2003) and performing a non-linear regression to determine the value of the exponent b. The regression yielded a value of $1\cdot35$ for b with $R^2 = 0\cdot85$. Rounding b upwards to $1\cdot4$, Equations 15 and 16 become

$$e_b = 0\cdot6 G^{1\cdot4} \tag{17}$$

$$\frac{U_b}{u} = 0\cdot6 G^{0\cdot4} \tag{18}$$

Figure 4 shows that Equation 17 is a good fit to the data where $\theta < 0\cdot1$, but that the data tend to plot above Equation 17 where $\theta \geq 0\cdot1$. The tendency for Equation 17 to underestimate e_b is reminiscent of Equation 12 underestimating s_b and is attributed to intergranular collisions which reduce U_b and inflate e_b. This explanation is supported by a positive correlation ($r = 0\cdot87$) between C_b and the difference between the computed and predicted values of e_b (i.e. log e_b minus predicted log e_b) (Figure 5).

That Equations 12 and 17 tend to underestimate s_b and e_b where $\theta \geq 0\cdot1$ is ascribed to Equation 8 being used to estimate U_b. Equation 8 was developed for flows with low bed shear stress ($\theta < 0\cdot1$) and overestimates U_b when it is applied to flows with medium to high bed shear stress ($\theta \geq 0\cdot1$). This overestimation of U_b, in turn, causes Equations
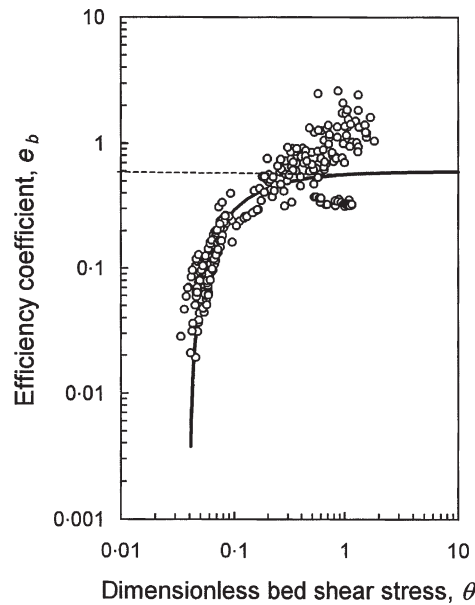
Figure 4. Graph of the efficiency coefficient against dimensionless bed shear stress. The line is Equation 17. U_b is calculated using Equation 8.
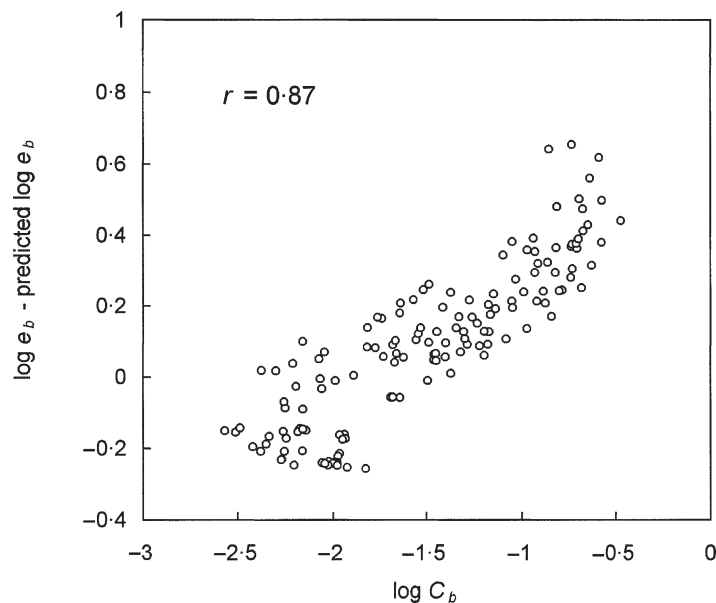
Figure 5. Graph of log e_b − predicted log e_b against log C_b for the 145 flows with $\theta \geq 0\cdot10$.

12 and 17 to underestimate s_b and e_b, as can be seen in Figures 2 and 4. This problem disappears, however, if the equation employed to estimate U_b applies to flows with mobile beds in both the saltation and sheet-flow regimes. Equation 18 is such an equation, and Figures 6 and 7 show that when it is used to estimate U_b, Equations 12 and 17 yield relatively unbiased estimates of s_b and e_b in both regimes. Further testing with other data sets is needed to establish the generality of Equation 18.
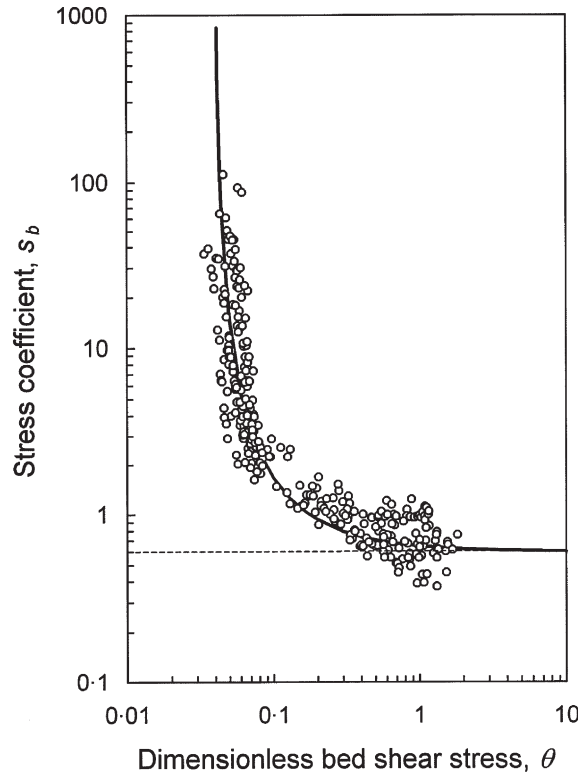
Figure 6. Graph of the stress coefficient against dimensionless bed shear stress. The line is Equation 12. U_b is calculated using Equation 18.
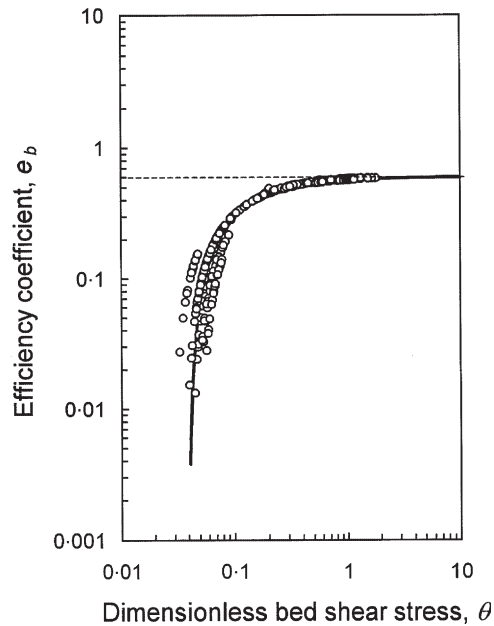
Figure 7. Graph of the efficiency coefficient against dimensionless bed shear stress. The line is Equation 17. U_b is calculated using Equation 18.

Bed-load Transport Equation

Equation

Rearranging the revised energy equation (i.e. Equation 11) and replacing s_b and e_b with their functional relations (Equations 12 and 17) yields the equation

$$\frac{i_b}{\omega} = \frac{e_b}{s_b} = G^{3.4} \tag{19}$$

Taking the first and last terms in this equation and multiplying them by ω produces the bed-load transport equation

$$i_b = \omega G^{3.4} \tag{20}$$

Figure 8 displays a graph of measured i_b against i_b predicted by Equation 20 for the 322 flume experiments in the present data set. The plotted points scatter symmetrically around the line of perfect agreement over six orders of magnitude. Clearly Equation 20 is a good predictor of i_b in both the saltation and the sheet-flow regimes.

It has been known for some time that i_b becomes proportional to ω at high shear stress (e.g. Colby, 1964, figure 16; Bagnold, 1973, p. 498; Leopold and Emmett, 1976, figure 1; Reid and Laronne, 1995, figure 3; Bridge, 2003, p. 61). However, Abrahams (2003) found that i_b is not just proportional to ω but where shear stress is high enough and bed load is being transported at capacity

$$i_b = \omega \tag{21}$$

This equality is explained in the section Transport Efficiency. In the meantime, a comparision of Equations 20 and 21 reveals that as G increases and approaches 1, Equation 20 reduces to Equation 21. Thus, Equation 21 is an asymptote that plots of (ω, i_b) approach as G increases. In the saltation regime i_b is sensitive to D, so flows transporting bed load of different sizes plot along separate curves below the $i_b = \omega$ line (Figure 9). The value of D associated with each
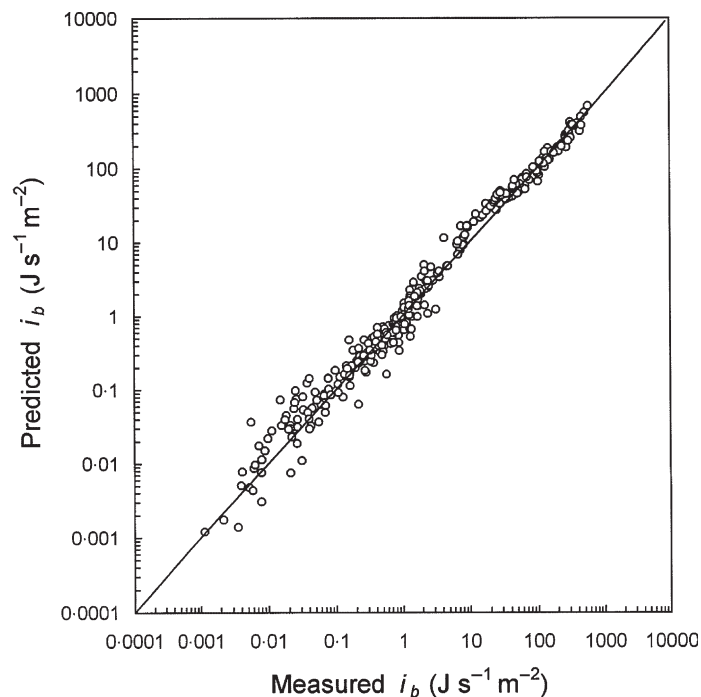
Figure 8. Graph of predicted i_b against measured i_b. The predictive equation is Equation 20.

curve increases from left to right. By contrast, in the sheet-flow regime, the entire bed is moving, and the immersed weight of the bed load is equal to the normal stress regardless of D. Consequently, i_b is insensitive to D (Wilson, 1987; Abrahams, 2003), and all the data plot along the $i_b = \omega$ line.

Boundaries

Abrahams (2003) concluded that bed-load transport by sheet flow conforms to and may be characterized by Equation 21, that is, $i_b/\omega = 1$. In actuality, Equation 21 or $i_b/\omega = 1$ defines the upper limit of a range of i_b/ω values that are associated with sheet flow. The lower limit of this range is a function of θ_c and θ_t and may be calculated from Equation 20. For example, if we assume that $\theta_c = 0.04$ and $\theta_t = 0.5$, the computed value of i_b/ω is 0.75. It follows that as flow intensity increases, i_b/ω increases and asymptotically approaches 1. When i_b/ω reaches 0.75, the mode of bed-load transport changes from saltation to sheet flow. Thus, $i_b/\omega = 0.75$ defines the lower boundary and $i_b/\omega = 1$ the upper boundary of the sheet-flow regime. Given that $i_b/\omega = G^{3.4}$ (Equation 20), it can be seen that these boundaries may also be defined in terms of G. For example, where $\theta_c = 0.04$ and $\theta_t = 0.5$, $G = 0.92$ defines the lower boundary and $G = 1$ the upper boundary of the sheet-flow regime. That the sheet-flow regime occupies a range of i_b/ω (and G) values means that Equation 21 does not fully define this regime. However, the range is so narrow and Equation 21 is so appealing in its simplicity that we recommend that this equation continue to be used to characterize and predict bed-load transport rates in this regime.

Transport Efficiency

That $i_b = \omega$ in Equation 21 does not mean that all the flow power in the sheet-flow regime is dissipated in the transport of bed load. As a measure of transport rate, i_b ($= W'U_b$) has the same dimensions as rate of doing work, but it is not a work rate because the force W' acts normal to the bed while the velocity U_b acts parallel to it. For the transport rate i_b to become a work rate ($= TU_b$), it must be multiplied by s_b ($= T/W'$). The efficiency coefficient e_b (i.e. the proportion of the flow power dissipated in the transport of bed load) can now be calculated using

$$e_b = i_b s_b / \omega \tag{13a}$$
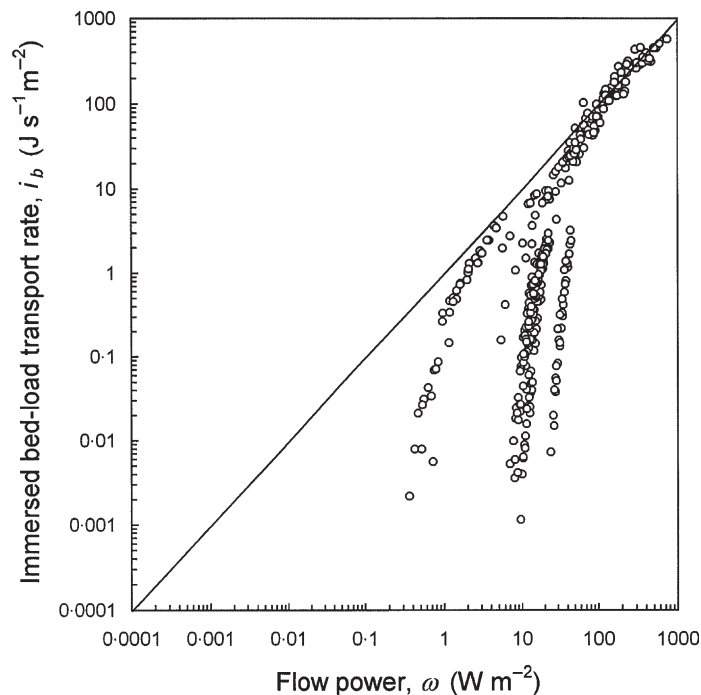
Figure 9. Graph of immersed bed-load transport rate against flow power. The line is Equation 21.

Substituting the bed-load transport equation (i.e. Equation 20) into Equation 13a yields

$$e_b = \frac{\omega G^{3 \cdot 4} s_b}{\omega} = G^{3 \cdot 4} s_b \tag{22}$$

which is a general expression for bed-load transport efficiency that applies in both the sheet-flow and saltation regimes. Equation 22 shows that the proportion of the total power supply that is dissipated transporting bed load increases with G and reaches a maximum of 0·6 when $G = 1$. This remarkably high coefficient of 0·6 (cf. Bagnold, 1966; Hanes and Bowen, 1985; Reid and Laronne, 1995, table 1) is attributed to changes in the type and frequency of intergranular collisions as bed shear stress increases.

Type and Relative Frequency of Grain Collisions

It is evident from the bed-load transport model presented above that the $s_b - G$ and $e_b - G$ relations are the key to understanding the bed-load transport equation (i.e. Equation 20). However, although it is clear that these two relations control Equation 20, it is not clear what controls these two relations.

As noted above, in bed-load transport grain collisions are either grain-to-grain (GG) or grain-to-bed (GB). On average one might expect the loss of streamwise momentum to be greater in a GB collision than in a GG one. In a GG collision, momentum is transferred from one moving grain to another. Because the grains are moving at similar speeds in approximately the same direction (i.e. downstream), little momentum is lost as a result of the collision. On the other hand, in a GB collision a moving grain strikes a stationary one and either stops or rebounds at a reduced velocity. In both scenarios, streamwise momentum is lost to the bed, and the loss is total where there is no rebound. Thus GG collisions conserve momentum better than GB ones, and the relative frequencies of these two types of collision might be expected to have an important influence on the bed-load transport rate.

With the object of predicting these relative frequencies, we define the property

$$P_g = \frac{N_{GG}}{N_{GG} + N_{GB}} \tag{23}$$

where P_g is the proportion of the total number of collisions per unit area per unit time that are GG collisions, and N_{GG} and N_{GB} are the numbers of GG and GB collisions, respectively, and then set out to determine the relation between P_g and G.

This relation is established with the aid of Leeder's (1979a) grain-collision model. Utilizing the gaseous kinetic theory, Leeder (1979a) formulated a theoretical model for the collisional behaviour of bed-load grains in saltation. In this model, Leeder (1979a) derived an expression for the mean free path length λ of a saltating grain between collisions, which he then compared with the average length of a saltation trajectory L at a given transport stage u_*/u_{*c}. If $\lambda = L$, the probability that a saltating grain will collide with another saltating grain in one saltation is 0·50 – that is, the probability of a GG collision is 0·50, which is the same as the probability of a GB collision. If $\lambda > L$, the probability of a GG collision is less than 0·50, and if $\lambda < L$, the probability of a GG collision is greater than 0·50.

Using the data from Abbott and Francis' (1977) experiments, Leeder (1979a, figure 4B) produced a graph of λ/L against transport stage. This graph shows that $\lambda/L = 1$ when $u_*/u_{*c} = 2$. Thus, Leeder (1979a) concluded that GG collisions occur at the same frequency as GB collisions when $u_*/u_{*c} = 2$. In other words, $P_g = 0 \cdot 50$ when $u_*/u_{*c} = 2$. Noting that $\theta/\theta_c = (u_*/u_{*c})^2$, then $u_*/u_{*c} = 2$ corresponds to $\theta/\theta_c = 4$ or $G = 0 \cdot 75$. Therefore, the relation between P_g and G must pass through the point (0·75, 0·5). In addition, logic dictates that the relation also passes through the points (0, 0) and (1, 1). Assuming the relation passing through these three points is a power function, then its equation is

$$P_g = G^{2 \cdot 4} \tag{24}$$

Although Leeder's (1979a) model is concerned with grain collisions, it depends on the relation between u_*/u_{*c} and λ/L developed from Abbott and Francis' (1977) flume experiments. Inasmuch as fluid lift would have been present in Abbott and Francis's experiments, its effect is included in Leeder's (1979a) model and therefore in Equation 24.

The $P_g - G$ relation (Equation 24) was derived independently of the bed-load transport equation (Equation 20), yet the exponent in the $P_g - G$ relation (Equation 24) is exactly 1 less than the exponent in the bed-load transport equation, and this difference is accounted for by the exponent of 1 in the $e_b - G$ relation (Equation 14). It is difficult to imagine this congruence occurring by chance. Consequently, it is concluded that this result strongly supports the

proposed bed-load transport model in general and the explanation for the $P_g - G$ relation based on the relative frequency of GG and GB collisions in particular.

The connections between Equations 20 and 24 are displayed in Figure 10 which, in a sense, is a summary of the bed-load transport model. The diagram contains the key equations of the model and shows how they are related to one another. It suggests that changes in G cause changes in P_g which, in turn, cause s_b and e_b to change. Thus, s_b and e_b are controlled by G via P_g. Inasmuch as $e_b/s_b = i_b/\omega$, i_b and ω must also be controlled by G via P_g.

Although a distinction may be drawn between uninterrupted saltation, interrupted saltation, and sheet flow, it appears that GG collisions conserve streamwise momentum better than do GB ones and that the mechanics of bed-load transport form a continuum along which P_g increases with G. As a result, the efficiency of bed-load transport e_b increases with P_g and approaches its maximum value of 0·6 as G approaches 1.

Alternative Forms

The bed-load transport equation developed here has its origins in Bagnold's (1966, 1973) energy equation. As a result, it uses i_b as the measure of bed-load transport rate and ω as the measure of flow intensity. However, this equation may also be written in the form

$$\phi_b = \theta^{1\cdot5} G^{3\cdot4} \frac{u}{u_*} \tag{25}$$

where $\phi_b = q_b/[(g\Delta D)^{0\cdot5}D]$ is the measure of bed-load transport rate (Einstein, 1950) and θ is the measure of flow intensity. Equation 20 is in fact the product of Equation 25 and $\rho(g\Delta D)^{1\cdot5}$, which means that although Equations 20 and 25 contain different variables, they are algebraically equivalent and give identical predictions. Thus, just as
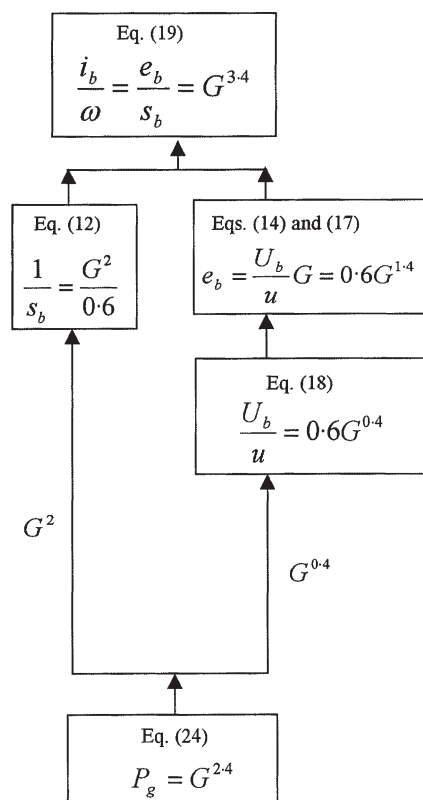
Figure 10. Flow diagram showing the paths whereby shear stress G controls s_b, e_b, and i_b/ω via P_g.

Equation 20 is a good predictor of i_b, Equation 25 is a good predictor of ϕ_b. This can be seen in Figure 11 where the data plot symmetrically around the line of perfect agreement over six orders of magnitude.

Furthermore, just as Equation 20 reduces to Equation 21, so Equation 25 reduces to

$$\phi_b = \theta^{1\cdot5}\frac{u}{u_*} \qquad (26)$$

in the sheet-flow regime (Abrahams, 2003). Equation 26 is of interest because many, if not most, equations for predicting the rate of bed-load transport in the sheet-flow regime (e.g. Wilson, 1966; Engelund, 1981; Jenkins and Hanes, 1998) have the form $\phi_b = k\theta^{1\cdot5}$, where the intercept k, whether it is a coefficient or a function, is a measure of flow resistance. Thus the right side of the equation has the attractive property of being a force-resistance ratio.

Conclusion

In this paper we develop a bed-load transport model that applies to rough turbulent open-channel flows transporting well sorted non-cohesive sediments over plane mobile beds. It is not the object of this model to predict bed-load transport rates in natural channels. Rather it is to develop an equation for predicting bed-load transport rates in simple two-dimensional flows over plane beds. These predicted bed-load transport rates may then be compared with measured rates in flows affected by bed forms, armouring, or limited sediment availability to assess the impact of these factors on bed-load transport rates.

This model is based on a revised version of Bagnold's (1966, 1973) basic energy equation in which the dynamic friction coefficient $\tan \alpha$ is replaced by a new coefficient termed the stress coefficient s_b. The stress coefficient is the tangential bed shear stress transmitted to the bed by grain contact and fluid drag divided by the immersed weight of the bed load which equals the normal dispersive stress due to grain collisions and fluid lift. The end-product of the model is the equation

$$i_b = \omega G^{3\cdot4} \qquad (20)$$
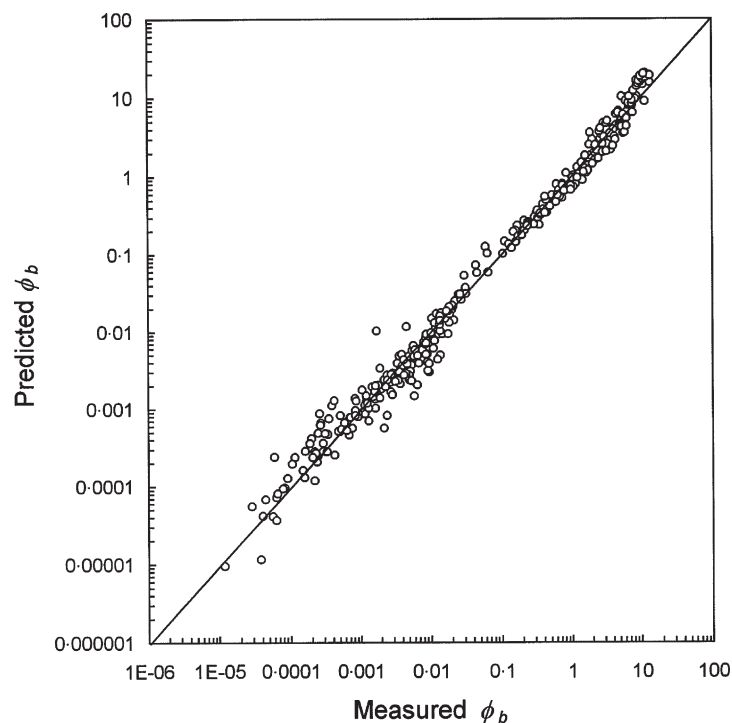
Figure 11. Graph of predicted ϕ_b against measured ϕ_b. The predictive equation is Equation 25.

where i_b is the immersed bed-load transport rate, ω is flow power, and G is a measure of sediment transport stage. This equation predicts i_b for a wide range of bed shear stress conditions that encompass both the saltation and sheet-flow regimes.

At high bed shear stress Equation 20 reduces to

$$i_b = \omega \tag{21}$$

which is the bed-load transport equation proposed for sheet flow by Abrahams (2003). This equation would seem to imply that all the available power is expended in the transport of bed load. But this is not the case, as i_b ($= W'U_b$) is a measure of transport rate in which the force W' acts normal to the bed while the velocity U_b acts parallel to it. To become a work rate, i_b must be multiplied by s_b ($= T/W'$). Then the proportion of ω that is dissipated in the transport of bed load is $i_b s_b/\omega$. In the sheet-flow regime where $i_b = \omega$, $s_b = \tan \alpha \approx 0.6$. Thus, it can be seen that up to 60 per cent of the available power may be expended in the transport of bed load. This remarkably high transport efficiency is attributed to two properties of bed-load transport: (1) the loss of streamwise momentum is generally much smaller in GG collisions than in GB ones; and (2) the relative frequency of GG collisions increases with bed shear stress.

There are many investigators (e.g. Simons and Senturk, 1992, pp. 548–549) who feel that the problem of predicting bed-load transport rates on plane beds has been solved. Their position is that equations capable of predicting bed-load transport rates on plane beds already exist in the literature and that, consequently, there is little merit in introducing yet another one. In defence of Equation 20, we would argue that this equation has several properties that distinguish it from other equations. For example:

(1) Equation 20 is the only bed-load transport equation that predicts the existence of the $i_b = \omega$ line (which coincides with the sheet-flow regime) and the convergence of the (i_b, ω) data on this line (which coincides with the saltation regime);
(2) without adjustments of any kind, Equation 20 provides unbiased estimates of bed-load transport rates in both the saltation and sheet-flow regimes;
(3) Equation 20 is extraordinarily simple in that it contains only one coefficient and this coefficient is the same in both the saltation and sheet-flow regimes.

The simplicity, parsimony, accuracy and generality of Equation 20 combine to make this equation uncommonly attractive as a predictor of bed-load transport rates on plane beds. In addition, Equation 20 provides unbiased estimates of bed-load transport rates in both the saltation and sheet-flow regimes. Given these attributes, Equation 20 would seem to be well suited to serve as a standard against which bed-load transport rates might be compared. Such a standard would be useful in identifying and quantifying the impact of various phenomena, such as bed forms, bed armouring and sediment availability, on bed-load transport rates. Employed in this way Equation 20 promises to be a valuable tool in the study of bed-load transport.

Acknowledgements

References

Abbott JE, Francis JRD. 1977. Saltation and suspension trajectories of solid grains in a water stream. *Philosophical Transactions of the Royal Society of London, Series A* **284**: 225–254.
Abrahams AD. 2003. A bed-load transport equation for sheet flow. *Journal of Hydraulic Engineering* **129**: 159–163.
Abrahams AD, Atkinson JF. 1993. Relation between grain velocity and sediment concentration in overland flow. *Water Resources Research* **29**: 3021–3028.
Allen JRL. 1985. *Principles of Physical Sedimentology*. George Allen and Unwin: London.
Aziz NM, Scott DE. 1989. Experiments on sediment transport in shallow flows in high gradient channels. *Hydrological Sciences Journal* **34:** 465–478.
Bagnold RA. 1954. Experiments on a gravity-free dispersion of large solid spheres in a Newtonian fluid under shear. *Proceedings of the Royal Society of London, Series A* **225:** 49–63.
Bagnold RA. 1956. The flow of cohesionless grains in fluids. *Transactions of the Royal Society of London, Series A* **249:** 235–297.
Bagnold RA. 1966. *An approach to the sediment transport problem from general physics*. US Geological Survey Professional Paper 422-I.

Bagnold RA. 1973. The nature of saltation and of 'bed-load' transport in water. *Proceedings of the Royal Society of London, Series A* **332**: 473–504.

Bridge JS. 2003. *Rivers and Floodplains: Forms, Processes and the Sedimentary Record*. Blackwell: Oxford.

Bridge JS, Bennett SJ. 1992. A model for the entrainment and transport of sediment grains of mixed sizes, shapes, and densities. *Water Resources Research* **28**: 337–363.

Bridge JS, Dominic DF. 1984. Bed load grain velocities and sediment transport rates. *Water Resources Research* **20**: 476–490.

Buffington JM, Montgomery D. 1997. A systematic analysis of eight decades of incipient motion studies, with special reference to gravel-bedded rivers. *Water Resources Research* **33**: 1993–2029.

Cheng NS. 1997. Simplified settling velocity formula for sediment particle. *Journal of Hydraulic Engineering* **123**: 149–152.

Cheng NS, Chiew YM. 1999. Analysis of initiation of sediment suspension from bed load. *Journal of Hydraulic Engineering* **125**: 855–861.

Chiew YM, Parker G. 1994. Incipient motion on non-horizontal slopes. *Journal of Hydraulic Research* **32**: 649–660.

Colby BR. 1964. *Discharge of sands and the mean-velocity relationships in sand-bed streams*. US Geological Survey Professional Paper 462-A.

Engelund F. 1981. *Transport of bed load at high shear stress*. Progress Report 53. Institute of Hydrodynamics and Hydraulic Engineering, Technical University of Denmark: Lyngby, Denmark.

Engelund F, Fredsoe J. 1982. Hydraulic theory of alluvial rivers. *Advances in Hydroscience* **13**: 187–215.

Engelund F, Hansen E. 1967. *A Monograph on Sediment Transport in Alluvial Sreams*. Teknisk Forlag: Copenhagen.

Fernandez Luque R, van Beek R. 1976. Erosion and transport of bed-load sediment. *Journal of Hydraulic Research* **14**: 127–144.

Fredsoe, J. 1993. Modelling of non-cohesive sediment transport processes in the marine environment. *Coastal Engineering* **21**: 71–103.

Gao P. 2003. *Mechanics of Bedload Transport in the Saltation and Sheetflow Regimes*. PhD dissertation, Department of Geography, University at Buffalo, Buffalo, NY.

Gao P, Abrahams AD. 2004. Bedload transport resistance in rough open-channel flows. *Earth Surface Processes and Landforms* **29**: 423–435.

Gomez B. 1991. Bedload transport. *Earth Science Reviews* **31**: 89–132.

Graf WH. 2000. Inception of sediment transport on steep slopes: discussion. *Journal of Hydraulic Engineering* **126**: 553.

Graf WH, Suszka L. 1987. Sediment transport in steep channels. *Journal of Hydroscience and Hydraulic Engineering* **5**: 11–26.

Guy HP, Simons DB, Richardson EV. 1966. *Summary of alluvial channel data from flume experiments, 1956–1961*. US Geological Professional Paper 462-I.

Hanes DM, Bowen AJ. 1985. A granular-fluid model for steady intense bed-load transport. *Journal of Geophysical Research* **90**(C5): 9149–9158.

Hill HM, Srinivasan VS, Tharakka EU. Jr. 1969. Instability of flat bed in alluvial channels. *Journal of the Hydraulics Division, Proceedings of the American Society of Civil Engineers* **95**: 1545–1558.

Jenkins JT, Hanes DM. 1998. Collisional sheet flows of sediments driven by a turbulent fluid. *Fluid Mechanics* **370**: 29–52.

Lau YL, Engel P. 1999. Inception of sediment transport on steep slopes. *Journal of Hydraulic Engineering* **125**: 544–547.

Leeder MR. 1979a. 'Bedload' dynamics: Grain-grain interactions in water flows. *Earth Surface Processes* **4**: 229–240.

Leeder MR. 1979b. 'Bedload' dynamics: Grain impacts, momentum transfer and derivation of a grain Froude number. *Earth Surface Processes* **4**: 291–295.

Leopold LB, Emmett WW. 1976. Bedload measurements, East Fork River, Wyoming. *Proceedings of the National Academy of Science, USA* **74**: 1000–1004.

McEwan IK, Jefcoate BJ, Willetts BB. 1999. The grain-fluid interaction as a self-stabillizing mechanism in fluvial bed load transport. *Sedimentology* **46**: 407–416.

Meade RH. 1985. Wavelike movement of bedload sediment, East Fork River, Wyoming. *Environmental Geology and Water Science* **7**: 215–225.

Middleton GV, Southard JB. 1984. *Mechanics of Sediment Movement*. SEPM: Tulsa, Oklahoma.

Nanson GC. 1974. Bedload and suspended load transport in a small steep mountain stream. *American Journal of Science* **274**: 471–486.

Nino Y, Garcia M. 1994. Gravel saltation 2. Modelling. *Water Resources Research* **30**: 1915–1924.

Nino Y, Garcia M. 1998a. Experiments on saltation of sand in water. *Journal of Hydraulic Engineering* **124**: 1014–1025.

Nino Y, Garcia M. 1998b. Using Lagrangian particle saltation observations for bedload sediment transport modelling. *Hydrological Processes* **12**: 1197–1218.

Nino Y, Garcia M, Ayala L. 1994. Gravel saltation 1. Experiments. *Water Resources Research* **30**: 1907–1914.

Nnadi FN, Wilson KC. 1992. Motion of contact-load particles at high shear stress. *Journal of Hydraulic Engineering* **118**: 1670–1684.

Nnadi FN, Wilson KC. 1995. Bed-load motion at high shear stress: dune washout and plan-bed flow. *Journal of Hydraulic Engineering* **121**: 267–273.

O'Leary SJ, Beschta RB. 1981. Bedload transport in an Oregon Coast Range stream. *Water Resources Bulletin* **17**: 886–894.

Pugh FJ, Wilson KC. 1999. Velocity and concentration distributions in sheet flow above plane beds. *Journal of Hydraulic Engineering* **125**: 117–125.

Reid I, Frostick LE. 1986. Dynamics of bedload transport in Turkey Brook, a coarse-grained alluvial channel. *Earth Surface Processes and Landforms* **11**: 143–155.

Reid I, Laronne LB. 1995. Bed load sediment transport in an ephemeral stream and a comparison with seasonal and perennial counterparts. *Water Resources Research* **31**: 773–781.

Reid I, Frostick LE, Layman JT. 1985. The incidence and nature of bedload transport during flood flows in coarse-grained alluvial channels. *Earth Surface Processes and Landforms* **10**: 33–44.

Rickenmann D. 1991. Hyperconcentrated flow and sediment transport at steep slopes. *Journal of Hydraulic Engineering* **117**: 1419–1539.

Schoklitsch A. 1914. *Uber Schleppkraft und Geschibebewegung*. Engelmann: Leipzig.

Sekine M, Kikkawa H. 1992. Mechanics of saltation grains, II. *Journal of Hydraulic Engineering* **118**: 536–558.

Seminara G, Solari L, Parker G. 2002. Bed load at low Shields stress on arbitrarily sloping beds: Failure of the Bagnold hypothesis. *Water Resources Research* **38**(11): 1249. DOI: 10.1029/2001 WR000681.

Simons DB, Senturk F. 1992. *Sediment Transport Technology*: *Water and Sediment Dynamics*. Water Resources Publications: Littleton, Colorado.

Smart GM. 1984. Sediment transport formula for steep channels. *Journal of Hydraulic Engineering* **110**: 267–276.

Song T, Chiew YM, Chin CO. 1998. Effect of bed-load movement on flow friction factor. *Journal of Hydraulic Engineering* **124**: 165–175.

Sumer BM, Kozakiewicz A, Fredsoe J, Deigaard R. 1996. Velocity and concentration profiles in sheet-flow layer of movable bed. *Journal of Hydraulic Engineering* **122**: 549–558.

van Rijn LC. 1982. Equivalent roughness of alluvial bed. *Journal of the Hydraulics Division, Proceedings of the American Society of Civil Engineers* **108**: 1215–1218.

van Rijn LC. 1984a. Sediment transport, Part I: Bed load transport. *Journal of Hydraulic Engineering* **110**: 1431–1456.

van Rijn LC. 1984b. Sediment transport, Part II: Suspended load transport. *Journal of Hydraulic Engineering* **110**: 1613–1641.

van Rijn LC. 1984c. Sediment transport, Part III: bedforms and alluvial roughness. *Journal of Hydraulic Engineering* **110**: 1733–1754.

van Rijn LC. 1993. *Principles of Sediment Transport in Rivers, Estuaries and Coastal Seas*. Aqua Publications: Amsterdam.

Wang Z, Chien N. 1987. Laminated load: its development and mechanism of motion. *International Journal of Sediment Research* **1**: 102–124.

Wang S, White WR. 1993. Alluvial resistance in transition regime. *Journal of Hydraulic Engineering* **119**: 725–741.

Whitehouse JS, Soulsby RL, Damgaard JS. 2000. Inception of sediment transport on steep slopes: discussion. *Journal of Hydraulic Engineering* **126**: 553–554.

Wiberg PL, Smith JD. 1989. Model for calculating bed load transport of sediment. *Journal of Hydraulic Engineering* **115**: 101–123.

Wijetunge JJ, Sleath JFA. 1998. Effects of sediment transport on bed friction and turbulence. *Journal of Waterway, Port, Coastal, and Ocean Engineering* **124**: 172–178.

Williams GP. 1970. *Flume width and water depth effects in sediment-transport experiments*. US Geological Survey Professional Paper 562-H.

Wilson KC. 1966. Bed-load transport at high shear stress. *Journal of the Hydraulics Division, Proceedings of the American Society of Civil Engineers* **92**: 49–59.

Wilson KC. 1987. Analysis of bed-load motion at high shear stress. *Journal of Hydraulic Engineering* **113**: 97–103.

Yen BC. 1991. Hydraulic resistance in open channels. In *Channel Flow Resistance: Centennial of Manning's Formula*, Yen BC (ed.). Water Resources Publications: Littleton, Colorado: 1–135.